

Nonlinear propagation of an intense Laguerre-Gaussian laser pulse in a plasma channel

Mingping Liu(刘明萍), Zhen Zhang(张震), Suhui Deng(邓素辉)
Citation: Chin. Phys. B, 2021, 30 (**5**): 055204. DOI: 10.1088/1674-1056/abd68c
Journal homepage: http://cpb.iphy.ac.cn; http://iopscience.iop.org/cpb

What follows is a list of articles you may be interested in

Laser-driven relativistic electron dynamics in a cylindrical plasma channel

Pan-Fei Geng(耿盼飞), Wen-Juan Lv(吕文娟), Xiao-Liang Li(李晓亮), Rong-An Tang(唐荣安), Ju-Kui Xue(薛具奎)
Chin. Phys. B, 2018, 27 (**3**): 035201. DOI: 10.1088/1674-1056/27/3/035201

K—P—Burgers equation in negative ion-rich relativistic dusty plasma including the effect of kinematic viscosity

A N Dev, M K Deka, J Sarma, D Saikia, N C Adhikary
Chin. Phys. B, 2016, 25 (**10**): 105202. DOI: 10.1088/1674-1056/25/10/105202

Enhanced laser-induced plasma channels in air

Yanlei Zuo(左言磊), Xiaofeng Wei(魏晓峰), Kainan Zhou(周凯南), Xiaoming Zeng(曾小明),Jingqin Su(粟敬钦), Zhihong Jiao(焦志宏), Na Xie(谢娜), Zhaohui Wu(吴朝辉)
Chin. Phys. B, 2016, 25 (**3**): 035203. DOI: 10.1088/1674-1056/25/3/035203

Relativistic degenerate effects of electrons and positrons on modulational instability of quantum ion acoustic waves in dense plasmas with two polarity ions

Liu Tie-Lu, Wang Yun-Liang, Lu Yan-Zhen
Chin. Phys. B, 2015, 24 (**2**): 025202. DOI: 10.1088/1674-1056/24/2/025202

Cylindrical and spherical Gardner solitons and double layers in a dusty electronegative nonthermal plasma with two-temperature electrons

T. Akhter, M. M. Hossain, A. A. Mamun
Chin. Phys. B, 2013, 22 (**7**): 075201. DOI: 10.1088/1674-1056/22/7/075201

Nonlinear propagation of an intense Laguerre–Gaussian laser pulse in a plasma channel*

Mingping Liu(刘明萍), Zhen Zhang(张震), and Suhui Deng(邓素辉)†

School of Information Engineering, Nanchang University, Nanchang 330031, *China*

(Received 2 September 2020; revised manuscript received 2 December 2020; accepted manuscript online 24 December 2020)

The nonlinear propagation of an intense Laguerre–Gaussian (LG) laser pulse in a parabolic preformed plasma channel is analyzed by means of the variational method. The evolution equation of the spot size is derived including the effects of relativistic self-focusing, preformed channel focusing, and ponderomotive self-channeling. The parametric conditions of the LG laser pulse and plasma channel for propagating with constant spot size, periodically focusing and defocusing oscillation, catastrophic focusing, and solitary waves are obtained. Compared with the laser pulse with fundamental Gaussian (FG) mode, it is found that the effect of vacuum diffraction is reduced by half and the effects of relativistic and wakefield focusing are decreased by a quarter due to the hollow transverse intensity profile of the LG laser pulse, while the effect of channel focusing is the same order of magnitude with that of the FG laser pulse. Thus, the matched condition for the intense LG laser pulse with constant spot size is released obviously, while the parameters of the laser and plasma for the existence of solitary waves nearly coincide with those of the FG laser pulse.

Keywords: nonlinear propagation, intense Laguerre–Gaussian laser pulse, wake-field effect, plasma channel

PACS: 52.38.−r, 52.35.Mw, 52.38.Hb **DOI:** 10.1088/1674-1056/abd68c

1. Introduction

The optical guiding of an intense laser pulse in plasma is very important to many promising applications, such as laser-driven accelerators,[1] harmonic generation,[2] laser confinement fusion,[3] and x/γ-ray radiation sources.[4] As we know, a laser pulse propagating in vacuum will diffract after a distance on the order of a Rayleigh length $Z_{\rm R} = \pi r_0^2/\lambda$, where r_0 is the laser spot size at focus and λ is the laser wavelength. However, an intense laser pulse in uniform plasmas can guide itself due to the relativistic self-focusing (RSF) when the laser power exceeds the critical power $P_{\rm c} = 17.4(\omega_0/\omega_{\rm p})^2$ (GW), where ω_0 is the laser frequency and $\omega_{\rm p}$ is the plasma frequency.[5] If the laser power is smaller than $P_{\rm c}$, laser diffraction will dominate over the RSF. In this case, a preformed plasma channel with a radially parabolic density profile can prevent laser diffraction and guide the latter propagating over many Rayleigh lengths,[6] which is beneficial to the above applications. In a realistic scenario, even if the laser power $P \geqslant P_{\rm c}$, GeV quasi-monoenergetic electron bunches can be obtained by increasing the acceleration length to a few centimeters in a laser guiding discharge capillary.[7–9] Recently, a striking result of electron bunch approaching 8 GeV has been measured in such channel-guided laser accelerator with more powerful laser systems.[10] Such high energy electron bunches provide a potential approach to produce high brightness x-ray and even γ-ray radiation sources.[11–13] Laser wake-field acceleration (LWFA) is the main acceleration mechanism for the generation of such energetic electron bunch and then wake field effects play a crucial role in electron acceleration like as the plasma channel.

In these experiments, laser pulses with fundamental Gaussian (FG) mode are usually used as drivers for propagating in a preformed plasma channel. It has been shown that the propagation characteristics of an intense laser pulse in a preformed plasma channel is strongly dependent on the interactions between the laser and plasma according to the principle of the refractive guiding.[5] When electrons quiver transversely in the electric field of an intense laser pulse, their mass increase relativistically and then the radial profile of the refraction index peaks on the propagating axis, which means that the plasma acts as a positive len. Consequently, the laser pulse focuses toward the axis, *i.e.*, the RSF occurs. A performed plasma channel with a radially parabolic density profile creates a refractive index profile with on-axis maximum, which yields the channel focusing (CF). The transverse ponderomotive force of an intense laser pulse can expel electrons away from the region where the laser intensity is the maximum, which gives rise to transverse gradient of the refractive index. This effect is well known as the ponderomotive self-channeling (PSC). All these nonlinearities discussed above present the focusing effects. Therefore, whether the laser pulse can realize guiding would mainly depend on the competition between the vacuum diffraction and the combined focusing effects of RSF, CF, and PSC. Many papers have investigated these focusing effects in the uniform plasma or preformed channel cases.[14–20] It has been found that the spot size of an laser pulse can evolve along the propagating axis

*Project supported by the National Natural Science Foundation of China (Grant Nos. 61665006 and 61865011) and the Natural Science Foundation of Jiangxi Province of China (Grant Nos. 20171ACB21018, 20161BAB212041, and 20162BCB23012).

†Corresponding author. E-mail: shdeng@ncu.edu.cn

© 2021 Chinese Physical Society and IOP Publishing Ltd

with constant, periodically focusing and defocusing oscillations, and catastrophic focusing. Further, Zhang *et al.* has investigated the existence conditions of solitary waves in a parabolic plasma channel.[21] The solitary waves are helpful to electron acceleration in the LWFA, because any perturbation of the solitary waves would lead to the wave breaking and realize the electron self-injection in the wake-field regime. Hong *et al.* found that when the laser length is on the order of plasma wavelength, a wake field will be excited efficiently and focus the laser pulse during its propagation forward.[22] Most of these results are based on the laser pulses with FG modes. In recent years, there has been an increasing interest on the laser pulses with Laguerre–Gaussian (LG) modes which have hollow transverse intensity profile and carry orbital angular momentum.[23–33] LG laser pulses drive donut-shaped wake fields whose field structure is capable of accelerating positrons and significantly enhances x/γ-ray generation.[23–26] Obviously, the dynamics of LG laser pulse propagating in a preformed plasma channel would definitely affect its application. In non-relativistic limit, the condition for the matched LG laser pulse in a preformed plasma channel is the same for all modes whether it includes the finite pulse length and group velocity dispersion or not.[6,34] However, electrons can be violently accelerated in the wake field regime driven by an intense laser pulse. Thus, these nonlinearities, such as group velocity dispersion, relativistic and wake-field effects, should be considered in analyzing the LG laser dynamics.

In this paper, we study the propagation characteristics of an intense LG laser pulse in a preformed plasma channel used by variational technique, including the combined effects of RSF, CF, and PSC. In order to effectively excite the wake field, the pulse length is defined as $L = \lambda_{\rm p}$ in our model,[1,5] where L and $\lambda_{\rm p}$ are the pulse length and plasma wavelength, respectively. The evolution equation of the LG laser spot size is obtained and then the conditions of laser and plasma channel parameters for propagating with constant spot size, periodically focusing, and defocusing oscillations, catastrophic focusing and solitary waves are identified in detail. All these nonlinear effects mentioned above are also illustrated numerically.

2. Evolution equation of laser spot size

The propagation along the z-direction of a linearly polarized laser pulse in a preformed plasma channel will be considered in our model. The density of the plasma channel is assumed with a profile of the form $n_{\rm ch}(r) = n_0 + \Delta n r^2/r_{\rm ch}^2$, where n_0 is the initial axial electron density, Δn and $r_{\rm ch}$ are the channel depth and radius, respectively. The normalized vector potential of the laser field is given by

$$\boldsymbol{a}(r,z,t) = \frac{1}{2}a(r,z,t)\exp[\mathrm{i}(kz-\omega t)]\hat{\boldsymbol{x}} + \mathrm{c.c.}, \tag{1}$$

where $\boldsymbol{a} = e\boldsymbol{A}/m_0c^2$ is the normalized amplitude of the vector potential of the laser field, e and m_0 are the charge and the rest mass of electron, c is the light velocity in vacuum, $\omega = ck/\beta_{\rm g}$ is the laser center frequency, $\beta_{\rm g} = v_{\rm g}/c$ is the normalized group velocity, $\hat{\boldsymbol{x}}$ is the unit vector along the x axis, and c.c. denotes the complex conjugate.

In the following, it is considered in the limit of weakly relativistic $|a|^2 < 1$ and under dense plasma $n_{\rm ch}/n_{\rm cr} < 1$, where $n_{\rm cr} = m_0\omega^2/4\pi e^2$ is the critical density. Starting from the Maxwell's equations and the relativistic cold electron fluid equations, to the order of $|a|^3$, using Coulomb gauge $\nabla\cdot\boldsymbol{a} = 0$, the coupling equations describing an intense laser pulse propagating in a preformed plasma channel can be written as[14,17,22]

$$\begin{aligned}&\Big[\nabla_\perp^2 + 2\mathrm{i}k\frac{\partial}{\partial z} + 2\frac{\partial^2}{\partial\xi\partial z} + (1-\beta_{\rm g}^2)\frac{\partial^2}{\partial\xi^2}\\&\quad - \Big(k^2 + k_{\rm p0}^2 - \frac{\omega^2}{c^2}\Big)\Big]a(r,z,\xi)\\&= -k_{\rm p0}^2\Big(\frac{|a|^2}{4} - \frac{\delta n}{n_0} - \frac{\Delta n r^2}{n_0 r_{\rm ch}^2} + \frac{\Delta n r^2}{n_0 r_{\rm ch}^2}\frac{|a|^2}{4}\Big)a(r,z,\xi),\end{aligned} \tag{2}$$

$$\Big[\frac{\partial^2}{\partial\xi^2} + \frac{k_{\rm p0}^2}{\beta_{\rm g}^2}\Big(1+\frac{\Delta n r^2}{n_0 r_{\rm ch}^2}\Big)\Big]\frac{\delta n}{n_0} = \frac{1}{4\beta_{\rm g}^2}\Big[\nabla_\perp^2 + \frac{\partial^2}{\partial\xi^2}\Big]|a|^2, \tag{3}$$

where $k_{\rm p0} = \omega_{\rm p0}/c$ is the plasma wave number, $\omega_{\rm p0} = \sqrt{4\pi n_0 e^2/m_0}$ is the electron plasma frequency, $\delta n/n_0 = (n - n_{\rm ch})/n_0$ is the normalized density perturbation, and the retarded system (z, $\xi = z - \beta_{\rm g}ct$) is introduced here. In deriving Eqs. (2) and (3), the term $\partial^2 a/\partial^2 z$ representing higher order diffraction is neglected in the limit $L \ll 2Z_{\rm R}$ and $L^2/r_0^2 \ll (1 + k_{\rm p0}^2 r_0^2/4 - k_{\rm p0}^2 r_0^2 a_0^2/16)$, where L is the pulse length. For a weakly relativistic laser pulse, the electron Lorentz factor, which is approximately $\gamma = \sqrt{1+|a|^2/2} \simeq 1 + |a|^2/4$, has been used to derive the source term of Eq. (2) and wake field generation in the linear regime can be obtained using the cold fluid equations, *i.e.*, Poisson equation, continuity equation, and fluid momentum equation. One can obviously see that equation (2) is the wave equation for the pulse envelop of the laser field and equation (3) is the perturbed density equation in the wake field region. The first, second, third, and fourth terms on the right-hand side of Eq. (2) are due to relativistic nonlinearity, wake field effect, plasma channel, and the coupling of relativistic nonlinearity with the plasma channel, respectively. Furthermore, the right-hand side of Eq. (3) represents the ponderomotive force of the laser pulse.

According to the propagation dynamics, a general solution to Eq. (2) is a LG mode, characterized by the mode numbers n and l, of the form

$$\begin{aligned}a(r,z,\xi) \;=\; & a_{\rm s}(z)\Big(\frac{\sqrt{2}r}{r_{\rm s}(z)}\Big)^l L_n^l\Big(\frac{2r^2}{r_{\rm s}(z)^2}\Big)\\&\times\exp\Big[\mathrm{i}\theta(z) - (1-\mathrm{i}\alpha(z))\frac{r^2}{r_{\rm s}(z)^2} + \mathrm{i}l\phi\Big]\\&\times\sin\big(\pi\xi/L\big),\quad (0\le\xi\le L),\end{aligned} \tag{4}$$

where L_n^l is the generalized Laguerre polynomial, ϕ is the polar angular coordinate, and $a_s(z)$, $\theta(z)$, $r_s(z)$, and $\alpha(z)$ are the real functions of the propagation distance z and represent the amplitude, phase shift, spot size, and curvature, respectively. For the sake of simplicity, the first order LG mode ($l=1$, $n=0$) is considered in our model, which has been used by most papers to study electron acceleration and radiation sources.[23–33] By inserting Eq. (4) into Eq. (3), the solution for the perturbed plasma density inside the pulse ($0 \le \xi \le L$) is given by

$$\begin{aligned}\frac{\delta n}{n_0} &= -\frac{a_s^2}{k_{p0}^2 r_s^2}\left[\frac{2r^2}{r_s^2} - \left(1-\frac{2r^2}{r_s^2}\right)^2\right]\exp\left(-\frac{2r^2}{r_s^2}\right)\\ &\times\left[1-\cos k_{p0}\xi + \frac{k_{p0}}{2}(\lambda_p-\xi)\sin k_{p0}\xi\right]\\ &-\frac{k_{p0}a_s^2}{16}\left(\frac{2r^2}{r_s^2}\right)\exp\left(-\frac{2r^2}{r_s^2}\right)(\lambda_p-\xi)\sin k_{p0}\xi. \quad (5)\end{aligned}$$

In deriving Eq. (5), the laser pulse with $L \sim \lambda_p$ and the normalized group velocity $\beta_g \simeq 1$ are assumed, wide channel approximation $k_{p0}r_{ch} > 1$, *i.e.*, the radial dependence of the plasma frequency can be neglected. The first and second terms on the right-hand side of Eq. (5) represent those induced by the transverse and longitudinal ponderomotive force of the laser pulse. By inserting Eqs. (4) and (5) into Eq. (2) and adopting the variational method,[16,17,35] we can obtain after some tedious algebra the following equations:

$$a_s = \frac{a_0 r_0}{r_s}, \quad (6)$$

$$\alpha = \frac{k r_s}{2}\frac{\partial r_s}{\partial z}, \quad (7)$$

$$\frac{\partial^2 r_s}{\partial z^2} = \frac{2}{k^2 r_s^3} - \frac{3k_{p0}^2 a_0^2 r_0^2}{128k^2 r_s^3} - \frac{k_{p0}^2 \Delta n r_s}{k^2 n_0 r_{ch}^2} - \frac{15a_0^2 r_0^2}{32k^2 r_s^5} - \frac{3\pi^2 a_0^2 r_0^2}{64k^2 r_s^3 L^2}, \quad (8)$$

where a_0 and r_0 are the initial ($z=0$) amplitude and spot size of the LG laser pulse, respectively. Considering the effects of relativistic, channel-coupling nonlinearity and wake field, one can obtain the evolution characteristics of the laser spot from Eqs. (6)–(8). Equation (6) indicates the power conservation relation $a_s^2 r_s^2 = a_0^2 r_0^2$. The first term on the right-hand side of Eq. (8) shows the vacuum diffraction, the second term represents the RSF, the third term yields the CF, the fourth and fifth terms present the wake-field effects induced by the transverse and longitudinal ponderomotive forces of the laser pulse, respectively. It obviously shows that the wake field also leads to the focusing of the LG laser pulse. Compared with the results of a FG laser pulse, such as Eq. (8) in Ref. [22], coefficient of the term of vacuum diffraction decreases by half and coefficients of the terms of the combined focusing also decrease by a quarter except the third term of the CF. Therefore, the hollow transverse intensity profile of the LG laser pulse significantly influences on its nonlinear propagation characteristics.

3. Propagation characteristics of the LG laser pulse

In the absence of wake field effect in Eq. (8), one can obtain that the normalized critical power for relativistic focusing using the LG laser pulse with the sinusoidal profile in the longitudinal direction is given by $P_c = 256/3$. If the trial function is a laser beam with FG mode then $P_c = 32$, which is corresponding to $17.4(k/k_{p0})^2$ GW in practical units.[5] To simplify the equation further, the dimensionless variables are introduced as $\tilde{z} = z/z_R$, $\tilde{r}_s = r_s/r_0$, and $\tilde{P} = P/P_c = 3k_{p0}^2 a_0^2 r_0^2/256$. The tildes are omitted in the following for convenience. Then, the normalized envelope equation for the laser spot size, *i.e.*, equation (8), can be rewritten as

$$\frac{\partial^2 r_s}{\partial z^2} = \left(\frac{1}{2} - \frac{3}{4}P\right)\frac{1}{r_s^3} - N_c r_s - \frac{15a_0^2}{128}\frac{1}{r_s^5}, \quad (9)$$

where $N_c = k_{p0}^2 r_0^4 \Delta n/4n_0 r_{ch}^2$ is a parameter related to the effect of preformed channel focusing. One should note that the effect of wake field induced by the longitudinal ponderomotive force has been incorporated into the effect of the RSF. Compared with the case of a FG laser pulse, *e.g.*, Eq. (9) in Ref. [22], one can obviously see that the effect of vacuum diffraction of the LG laser pulse is reduced by half, the CF has the same order of magnitude as the result of the FG laser pulse and the other combined focusing is significantly reduced by a quarter.

With the initial conditions $r_s|_{z=0} = 1$ and $\partial r_s/\partial z|_{z=0} = 0$, integrating Eq. (9) once yields

$$\frac{1}{2}\left(\frac{\partial r_s}{\partial z}\right)^2 + V(r_s) = 0, \quad (10)$$

where

$$V(r_s) = \frac{1}{4}\left(1-\frac{3P}{2}\right)\frac{1}{r_s^2} + \frac{1}{2}N_c r_s^2 - \frac{15a_0^2}{512}\frac{1}{r_s^4} - V_0, \quad (11)$$

$$V_0 = \frac{1}{4}\left(1-\frac{3P}{2}\right) + \frac{1}{2}N_c - \frac{15a_0^2}{512}. \quad (12)$$

Equation (10) has the same form of an energy equation for a particle in a potential well $V(r_s)$. Here, r_s has the role of the space coordinate and z is the "time". Thus, it is more instructive to discuss the solution of Eq. (10) according to the value of the potential $V(r_s)$, which in turn depends on the initial laser and plasma parameters.

We first analyze the potential function $V(r_s)$. By solving $V(r_s) = 0$, one can obtain three solutions as

$$r_{s1} = 1, \quad (13)$$

$$r_{s2} = [(N_p + \sqrt{N_p^2 - 15360N_c a_0^2})/512N_c], \quad (14)$$

$$r_{s3} = [(N_p - \sqrt{N_p^2 - 15360N_c a_0^2})/512N_c], \quad (15)$$

where $N_p = 128 - 192P - 15a_0^2$. The relations among the three roots intensively depend on the initial laser and plasma param-

eters. It is convenient to define three thresholds $P_{\rm th1} = (128 - 15a_0^2 - 32a_0\sqrt{15N_{\rm c}})/192$, $P_{\rm th2} = (64 - 15a_0^2 - 128N_{\rm c})/96$, and $N_{\rm th} = 15a_0^2/256$. It should note that when $N_{\rm c} = N_{\rm th}$, one can get the critical condition $P_{\rm th1} = P_{\rm th2}$. Thus, we can obtain the following results about the relations of the three roots as: (i) if $P > P_{\rm th1}$, $V(r_{\rm s}) = 0$ has only one real root, *i.e.*, $r_{\rm s1} = 1$; (ii) if $P = P_{\rm th1}$ and $N_{\rm c} = N_{\rm th}$, $V(r_{\rm s}) = 0$ has triple real roots, *i.e.*, $r_{\rm s1} = r_{\rm s2} = r_{\rm s3} = 1$; (iii) if $P = P_{\rm th1}$ and $N_{\rm c} > N_{\rm th}$, the roots are $r_{\rm s1} = 1$ and $r_{\rm s2} = r_{\rm s3} = (\sqrt{15}a_0/16\sqrt{N_{\rm c}})^{1/2} < 1$; (iv) if $P = P_{\rm th1}$ and $N_{\rm c} < N_{\rm th}$, the roots are $r_{\rm s1} = 1$ and $r_{\rm s2} = r_{\rm s3} = (\sqrt{15}a_0/16\sqrt{N_{\rm c}})^{1/2} > 1$; (v) if $P < P_{\rm th2}$, $V(r_{\rm s}) = 0$ has three unequal real roots, *i.e.*, $r_{\rm s3} < r_{\rm s1} < r_{\rm s2}$; (vi) if $P = P_{\rm th2}$ and $N_{\rm c} > N_{\rm th}$, the roots are $r_{\rm s1} = r_{\rm s2} = 1$ and $r_{\rm s3} < 1$; (vii) if $P = P_{\rm th2}$ and $N_{\rm c} < N_{\rm th}$, the roots are $r_{\rm s1} = r_{\rm s3} = 1$ and $r_{\rm s2} > 1$; (viii) if $P_{\rm th2} < P < P_{\rm th1}$ and $N_{\rm c} > N_{\rm th}$, $V(r_{\rm s}) = 0$ has three unequal real roots, *i.e.*, $r_{\rm s3} < r_{\rm s2} < r_{\rm s1}$; (ix) if $P_{\rm th2} < P < P_{\rm th1}$ and $N_{\rm c} < N_{\rm th}$, $V(r_{\rm s}) = 0$ has three unequal real roots, *i.e.*, $r_{\rm s1} < r_{\rm s3} < r_{\rm s2}$. For the sake of clarity, the evolutions of potential well $V(r_{\rm s})$ with the spot size $r_{\rm s}$ in the cases (i)–(ix) are depicted corresponding to Figs. 1(a)–1(i), respectively. One can clearly see the relations among the three roots according to the different laser power P and channel parameter $N_{\rm c}$. Therefore, it is easily obtain the propagation characteristics of a LG laser pulse propagating in a plasma channel from Fig. 1.

First of all, we discuss the condition for a matched (nonevolving) spot size of the LG laser pulse in the plasma channel. Only case (vi) mentioned above can ensure the test particle rest in the potential well $V(r_{\rm s})$ as shown in Fig. 1(f). Thus, if the initial laser and plasma parameters satisfy $P = P_{\rm th2}$ and $N_{\rm c} > N_{\rm th}$, the spot size $r_{\rm s} = 1$ will retain during the propagation of the LG laser pulse in the plasma channel. Second, the test particle will be unstable and eventually move boundlessly to the position $r_{\rm s} \to 0$, which can occur in the cases (i), (ii), (iv), and (ix), respectively. In this case, the spot size will be focused catastrophically and contracted to a geometric point. It should be pointed that the singularity will never occur since the laser intensity will be increased infinitely, which is beyond the weakly relativistic limit of our model. According to the parameter conditions of cases (i), (ii), (iv), and (ix), one can obtain the comprehensive parameter regions for catastrophic focusing, *i.e.*, $P > P_{\rm th1}$ for any $N_{\rm c}$ and $P_{\rm th2} < P \leq P_{\rm th1}$ for $N_{\rm c} \leq N_{\rm th}$. Third, one can find from Figs. 1(e) and 1(h) that the test particle will oscillate back and forth between $r_{\rm s1}$ and $r_{\rm s2}$. So the structure of the spot size $r_{\rm s}$ is a train of finite amplitude waves with finite wavelength. The test particle will perform periodically defocusing oscillation in the case (v) whereas perform periodically focusing oscillation in the case (viii). Last but not least, in cases (vii) and (iii), the test particle initially lies in or moves to a critical point. It is very interesting to discuss the two critical cases for the propagation of LG laser pulse in a preformed plasma channel.

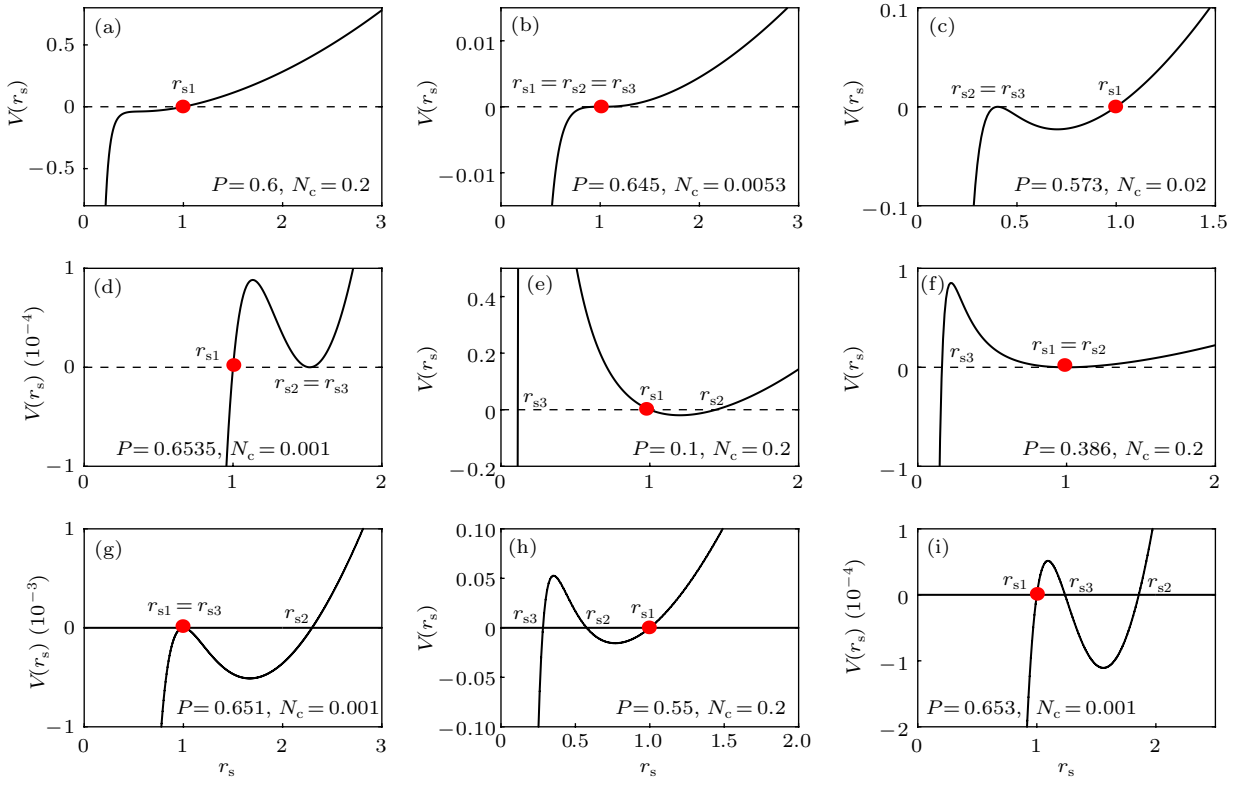


Fig. 1. Potential well $V(r_{\rm s})$ as a function of $r_{\rm s}$. Panels (a)–(i) correspond to the enumerated cases (i)–(ix) in the paper discussed above $r_{\rm s1}$, $r_{\rm s2}$, and $r_{\rm s3}$ are the three roots of $V(r_{\rm s}) = 0$. The red point in each figures represents the initial position of a test particle with $r_{\rm s} = 1$ and $\partial r_{\rm s}/\partial z = 0$. The normalized laser amplitude is $a_0 = 0.3$ for all cases.

According to the nonlinear dynamics theory, equation (9) can be reduced to the following autonomous system's equations:

$$\frac{\partial r_s}{\partial z} = u, \tag{16}$$

$$\frac{\partial u}{\partial z} = -V'(r_s). \tag{17}$$

Here $V(r_s)$ has been taken once the r_s derivative in Eq. (17). In the case (vii), the test particle initially lies in the critical point (1, 0), which is one of the two fixed points of the autonomous system. The eigenvalues of the linearized equations of Eqs. (16) and (17) are $\eta_{1,2} = \pm\sqrt{-V''}|_{r_s=1}$. Since the potential well $V(r_s)$ has a maximum at $r_s = 1$, $V''|_{r_s=1} < 0$ holds. Thus, one of the eigenvalues is a positive real number while the other is a negative real number. Therefore, the critical point (1, 0) is a saddle point and equation (9) has solitary wave solution in the case (ix). Similarly, in the case (iii), it can prove that the point $(r_{s2}(=r_{s3}),0)$ is also a saddle point. The test particle with the initial position (1, 0) lies in the homoclinic orbit passing through the saddle point $(r_{s2},0)$ since $H(r_{s2},0) = H(1,0)$, where H is the Hamiltonian function of the autonomous system. Hence, equation (9) also has solitary wave solutions in the case (iii). Consequently, it exists solitary waves for the LG laser pulse in the appropriate parameters of laser and plasma. From cases (iii) and (vii), one can obtain that the initial parameters of the LG laser pulse and plasma channel for the existence of solitary waves should satisfy as $P = P_{th1}$ for $N_c > N_{th}$ and $P = P_{th2}$ for $N_c < N_{th}$.

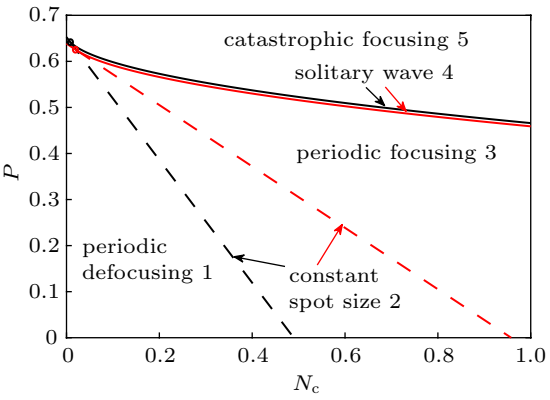


Fig. 2. Propagation characteristics of a LG laser pulse (black curves) and a FG laser pulse (red curves) for $a_0 = 0.3$. The circles correspond to the critical parameters N_{th}. The solid curves 4 represent the parameters of the existence of the solitary waves, while the dashed curves 2 denote the propagation of laser pulse with constant spot size. There are three regions, which correspond periodically defocusing oscillations (region 1), periodically focusing oscillations (region 3), and catastrophic focusing (region 5). The results of the FG laser pulse have calculated according to the formulas of Ref. [22].

In order to get the full view of the propagation characteristics of the intense LG laser pulse, the initial parameters of laser and plasma channel for each cases discussed above are plotted in Fig. 2 (black curves). For comparison, the propagation characteristics of a FG laser pulse in a preformed channel are also shown in Fig. 2 (red curves). The solid curves 4 are the critical power of the laser pulse for the existence of the solitary waves under different the channel parameter N_c, and the dashed curves 2 denote the laser power for its propagation with constant spot size. The two types of curves classify the N_c–P plane with three regions corresponding to the periodically defocusing oscillation (region 1), periodically focusing oscillation (region 3) and catastrophic focusing (region 5), respectively. As expected, the effects of relativistic, channel-coupling nonlinearity and wake field greatly release the total critical power P for the laser focusing, which is far smaller than 1. It is obviously seen from Fig. 2 that the critical power of the LG laser pulse for the existence of the solitary waves almost coincides with that of the FG laser pulse, while the laser power for its propagation with constant spot size in the case of the LG laser pulse is decreased remarkably compared with the case of the FG laser pulse. When $N_c = 0.5$, the powers for the existence of the solitary waves are 0.525 for the LG laser pulse and 0.515 for the FG laser pulse, respectively. However, the power for the propagation with constant spot size is very weak, *i.e.*, $P \simeq 0$, in the case of the LG laser pulse, which is more less than that ($P = 0.305$) in the case of the FG laser pulse. Therefore, one can note that there is a overlapping area between the periodic focusing region of the LG laser pulse and the periodic defocusing region of the FG laser pulse.

4. Numerical results and discussion

In this section, the propagation characteristics of the LG laser pulse in a performed plasma channel are numerically investigated according to Eq. (9), which is solved using the fourth-order Runge–Kutta method with the parameters presented in Fig. 1 and the initial conditions $r_s|_{z=0} = 1$ and $\partial r_s/\partial z|_{z=0} = 0$. The evolution of laser spot size r_s and amplitude a_s with the propagation distance z will be shown in the following Figs. 3–5 for the cases of constant spot size, catastrophic focusing, periodically focusing (or defocusing) oscillation, and solitary waves, respectively.

It can be seen from Eq. (9) that the propagation characteristics of the LG laser pulse strongly depend on the competition between the vacuum diffraction and the combined focusing effects of relativistic, channel-coupling nonlinearity, and wake field. When the effect of the vacuum diffraction is exactly canceled by the combined focusing effects, the equilibrium solution with constant spot size r_s and constant amplitude a_s are shown in the solid curves of Fig. 3 corresponding to the case (vi) of Fig. 1. If the combined focusing effects significantly overwhelm the vacuum diffraction, the catastrophic focusing will happen. One can see the cases of the catastrophic focusing plotted in Fig. 3 with the dashed curves, dotted curves and dash–dotted curves, which correspond to the

cases of Figs. 1(a), 1(d), and 1(i), respectively. With the nearly same laser power P, the spot size r_s of the case of Fig. 1(a) is focused catastrophically more faster than those cases of Figs. 1(d) and 1(i) because of the higher channel parameter N_c. As mentioned early, the catastrophic focusing will never occur since the laser intensity will increase infinitely when the spot size is focused to zero. Then, the effects of higher-order relativistic nonlinearities and other terms will prevent the spot size collapse in the real laser-plasma interactions. Actually, the high-intense laser pulse ($a_0 \geq 1$) will expel local plasma electrons and create an electron-free blowout. This effect will lead to the diffracting propagation for the laser pulse as in the vacuum.[36,37] Even so, it is still out of the weakly relativistic limit used in our model.

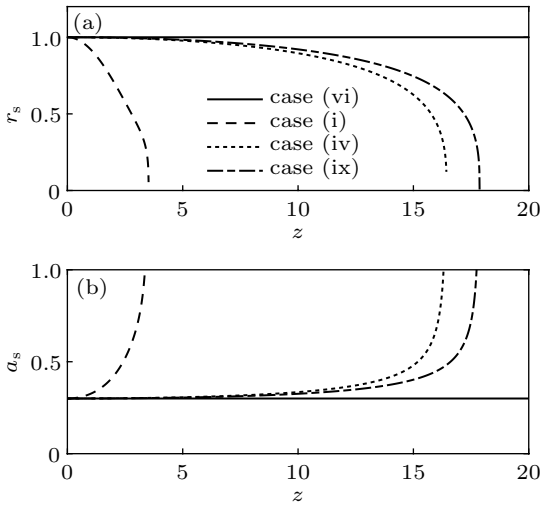


Fig. 3. The evolution of laser spot size r_s (a) and amplitude a_s (b) with the propagation distance z. The propagation characteristics of the LG laser pulse with constant spot size are plotted with the parameters of Fig. 1(f) (solid curve), while the cases of catastrophic focusing are plotted with the parameters of Fig. 1(a) (dashed curve), (d) (dotted curve), and (i) (dash–dotted curve).

If the initial parameters of laser and plasma are chosen as in region 1 of Fig. 2, the periodically defocusing oscillations will occur as shown in Figs. 4(a) and 4(c) responding to the case of Fig. 1(e). In this region, the combined focusing effects are weaker than the vacuum diffraction in the beginning, and the laser spot size in turn increases at first, which can be verified by r_s with greater than 1 in Fig. 4(a). With the increase of the spot size, the CF will be enhanced but the vacuum diffraction becomes weaker. Then, the defocusing behavior of the spot size will be prevented and it will decrease after reaching a peak. Thus, the periodically defocusing oscillations of the laser spot size will form as shown in Fig. 4(a). In the region 3 of Fig. 2, with the parameters of laser and plasma in this region, *e.g.* the the case (viii) of Fig. 1, the laser spot size decreases at first and will be less than 1, which leads to enhancing the vacuum diffraction but decreasing the CF. Thus, the periodically focusing oscillations can build as shown in Figs. 4(b) and 4(d).

The propagation characteristics of solitary waves are presented in Fig. 5. One can see that the homoclinic orbits in r_s–$\partial r_s/\partial z$ plane are depicted in Figs. 5(a) and 5(b) corresponding to the parameters of Figs. 1(c) and 1(g), respectively. It means that the evolution of the spot size r_s and amplitude a_s with the propagation distance z will be solitary waves. However, in general it is hard to get the exact solutions of the solitary wave for Eq. (9) since the numerical error is unavoidable. Hence, a train of solitary-like waves of the spot size r_s, of course amplitude a_s, are shown in Figs. 5(c)–5(f). It should note that in the case of Fig. 1(c), the initial spot size is not at a saddle point and a solitary-like structure is formed at first, and then the spot size keeps constant for a long distance about $7Z_R$. However, in the case of Fig. 1(g), the spot size initially lies on a saddle point and in turn keeps constant at first for a longer distance about $150Z_R$. It is worth pointing out that the solitary-like waves have the focusing effect in Figs. 5(a), 5(c), and 5(e) because of the higher channel focusing, while the solitary-like waves have the defocusing effect in Figs. 5(b), 5(d), and 5(f).

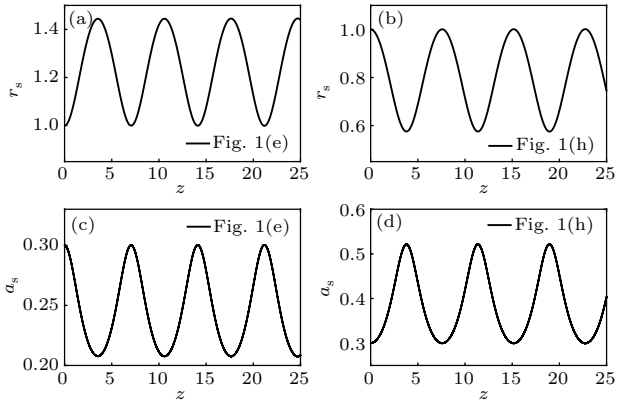


Fig. 4. The evolution of laser spot size r_s (a) and amplitude a_s (c) shows the periodically defocusing oscillation with the parameters of Fig. 1(e). The evolution of laser spot size r_s (b) and amplitude a_s (d) shows the periodically focusing oscillation with the parameters of Fig. 1(h).

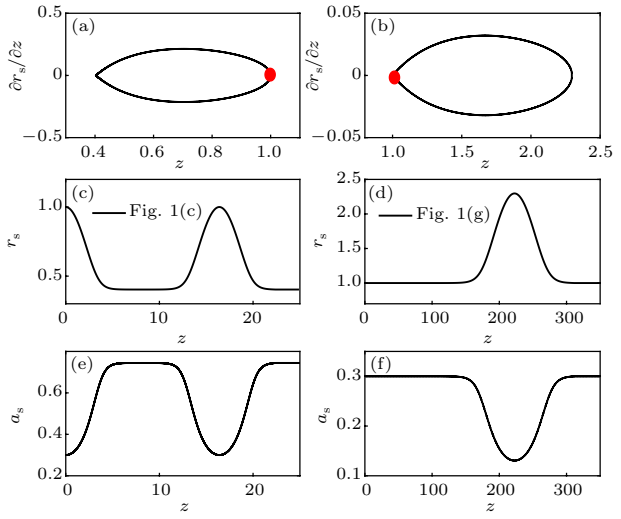


Fig. 5. Propagation characteristics of solitary-like waves corresponding to the cases of Fig. 1(c) (left column) and 1(g) (right column). (a) and (b) Orbits on the phase plane r_s–$\partial r_s/\partial z$, the initial position is marked in red; (c) and (d) the evolution of the laser spot size r_s with the propagation distance z; (e) and (f) the evolution of the laser amplitude a_s with the propagation distance z.

In order to further understand the influence of the hollow transverse intensity profile of the LG laser pulse on its propagation characteristics, it is necessary to investigate the behaviors of the spot size of the LG and FG laser pulses with the same initial parameters. Figure 6 shows the evolution of the spot size r_s of the LG (solid curves) and FG (dashed curves) laser pulses with the same parameters of laser power and plasma channel in the different regions of Fig. 2, *i.e.*, $P = 0.2$ and $N_c = 0.2$ in region 1, $P = 0.2$ and $N_c = 0.5$ in the overlapping region, $P = 0.4$ and $N_c = 0.5$ in the region 3, and $P = 0.6$ and $N_c = 0.8$ in the region 5. In region 1 of Fig. 2, both of the LG and FG laser pulses perform periodically defocusing oscillations as shown in Fig. 6(a). However, the effect of vacuum diffraction of the LG laser pulse is weaker than that of the FG laser pulse and then the spot size of the latter increases to the peak about 2.05, close to 1.6 times the peak value of the former. When the channel parameter N_c increases to 0.5, *i.e.*, in the overlapping region of Fig. 2, the combined focusing effects overwhelm the vacuum diffraction effect for the LG laser pulse and it in turn performs periodically focusing oscillations as shown in Fig. 6(b). However, due to the stronger vacuum diffraction, the FG laser pulse still remains the periodically defocusing oscillations but with the smaller amplitude of oscillation. In region 3 of Fig. 2, the combined focusing continually overwhelms the vacuum diffraction for the LG laser pulse and then its oscillation amplitude is further enhanced as shown in Fig. 6(c). Due to the enhanced laser power, the FG laser pulse converts to present periodically focusing oscillations with the smaller amplitude of oscillation. When the parameters of laser power and plasma channel locate in the region 5 of Fig. 2, the focusing characteristics of the LG and FG laser pulses coincide with each other except the spot size r_s close to 0 as shown in Fig. 6(d), which will never occur.

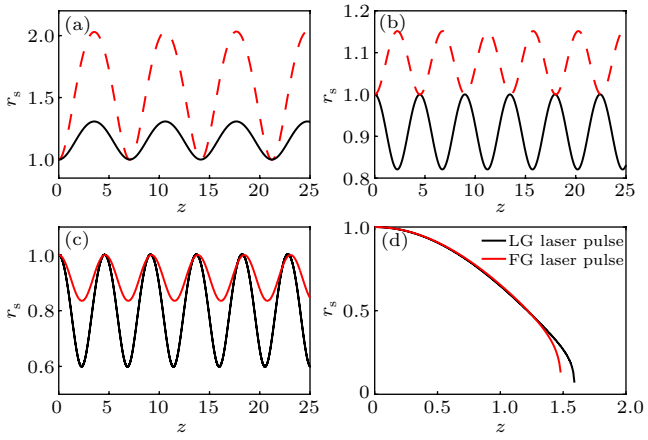


Fig. 6. The evolution of spot size r_s with propagation distance z for the LG (black solid curves) and FG (red dashed curves) laser pulses. The parameters of laser pulse and plasma channel are (a) $P = 0.2$ and $N_c = 0.2$ in region 1 of Fig. 2, (b) $P = 0.2$ and $N_c = 0.5$ in the overlapping region of Fig. 2, (c) $P = 0.4$ and $N_c = 0.5$ in the region 3 of Fig. 2, and (d) $P = 0.6$ and $N_c = 0.8$ in the region 5 of Fig. 2, respectively.

5. Conclusion

In a summary, the propagation characteristics of an intense LG laser pulse in a performed plasma channel are investigated, which takes into account the combined effects of relativistic, channel-coupling nonlinearity, and wake field. An evolution equation of the laser spot size is derived by means of the variational method. It is proved that the LG laser pulse can propagate with constant, periodically defocusing and focusing oscillations, catastrophic focusing, and solitary waves, respectively. The behaviors of the laser spot size and amplitude strongly depend on the initial parameters of the LG laser pulse and plasma channel, *i.e.*, laser amplitude a_0, laser power P, and channel parameter N_c. Comparing with the propagation characteristics of a FG laser pulse, the effect of the vacuum diffraction is reduced by half and the effects of relativistic and wake-field focusing are decreased by one quarter because of the hollow transverse intensity profile of the LG laser pulse. However, the CF effect is the same order of magnitude with that of the FG laser pulse. Correspondingly, the matched condition for the LG laser pulse with constant spot size is reduced obviously, while the parameters of the laser and plasma for the existence of solitary waves nearly coincides with those of the FG laser pulse. Therefore, the characteristic region of the periodically defocusing oscillation is enlarged compared with the case of the FG laser pulse and the characteristic region of the periodically focusing oscillation in turn is reduced.

Our work shows that the propagation characteristics of the LG laser pulse are remarkably different from those of the FG laser pulse in a preformed plasma channel. The results could be useful for the LG laser-plasma acceleration and further new sources of radiation. It should notice that when the laser power and channel parameter exceed the condition for the existence of solitary waves, the catastrophic focusing of the laser with intensity increasing infinitely and spot size focused to be zero will occur, which is out of the weakly relativistic limit in our model. Actually, our model is still valid for mildly relativistic limit of the laser intensity, *i.e.*, $|\, a \,| \sim 0.6$, according to the approximation $\sqrt{1+|a|^2/2} \simeq 1+|a|^2/4$. When the normalized laser amplitude is enhanced to one or even more, an electron cavitation can be formed around the propagation axis and then the relativistic propagation of a high-intense LG laser pulse in a preformed plasma channel play an important role for electron acceleration and the generation of radiation sources, which would be investigated in the near future.

References

[1] Tajima T D and Dawson J M 1979 *Phys. Rev. Lett.* **43** 267
[2] Milchberg H M, Durfee C G and McIlrath T J 1995 *Phys. Rev. Lett.* **75** 2494
[3] Tabak M, Hammer J, Glinsky M E, Kruer W L, Wilks S C, Woodworth J, Campbell E M, Perry M D and Mason R J 1994 *Phys. Plasmas* **1** 1626
[4] Corde S, Ta Phuoc K, Lambert G, Fitour R, Malka V, Rousse A, Beck A and Lefebvre E 2013 *Rev. Mod. Phys.* **85** 1

[5] Esarey E, Schroeder C B and Leemans W P 2009 *Rev. Mod. Phys.* **81** 1229

[6] Esarey E and Leemans W P 1999 *Phys. Rev. E* **59** 1082

[7] Leemans W P, Nagler B, Gonsalves A J, Tóth Cs, Nakamura K, Geddes C G R, Esarey E, Schroeder C B and Hooker S M 2006 *Nat. Phys.* **2** 696

[8] Wang X, Zgadzaj R, Fazel N, Li Z, Yi S A, Zhang X, Henderson W, Chang Y Y, Korzekwa R, Tsai H E, Pai C H, Quevedo H, Dyer G, Gaul E, Martinez M, Bernstein A C, Borger T, Spinks M, Donovan M, Khudik V, Shvets G, Ditmire T and Downer M C 2006 *Nat. Commun.* **4** 1988

[9] Leemans W P, Gonsalves A J, Mao H S, Nakamura K, Benedetti C, Schroeder C B, Toth C, Daniels J, Mittelberger D E, Bulanov S S, Vay J L, Geddes C G and Esarey E 2014 *Phys. Rev. Lett.* **113** 245002

[10] Gonsalves A J, Nakamura K, Daniels J, Benedetti C, Pieronek C, de Raadt T C H,Steinke S, Bin J H, Bulanov S S, van Tilborg J, Geddes C G R, Schroeder C B, Toth C,Esarey E, Swanson K, Fan-Chiang L, Bagdasarov G, Bobrova N, Gasilov V, Korn G, Sasorov P and Leemans W P 2019 *Phys. Rev. Lett.* **122** 084801

[11] Kneip S, McGuffey C, Martins J L, Martins S F, Bellei C, Chvykov V, Dollar F, Fonseca R, Huntington C, Kalintchenko G, Maksimchuk A, Mangles S P D, Matsuoka T, Nagel S R, Palmer C A J, Schreiber J, Phuoc K, TaThomas A G R, Yanovsky V, Silva L O, Krushelnick K and Najmudin Z 2010 *Nat. Phys.* **6** 980

[12] Tan F, Zhu B, Han D, Xin J T, Zhao Z Q, Cao L F, Gu Y Q and Zhang B H 2014 *Chin. Phys. B* **23** 034104

[13] Chen L M, Lu X, Li D Z and Li Y F 2018 *Chin. Phys. B* **27** 074101

[14] Esarey E,Sprangle P, Krall J and Ting A 1996 *IEEE Trans. Plasma Sci.* **24** 252

[15] Liu M, Guo H, Zhou B, Li W, Li B and Wu G 2004 *Phys. Lett. A* **333** 478

[16] Jha P, Malviya A and Upadhyay A K 2010 *Laser Part. Beams* **28** 245

[17] Zhang S, Hong X R, Wang H Y and Xie B S 2011 *Phys. Lett. A* **375** 4022

[18] Liu M P, Liu B B, Liu S Q, Zhang F Y and Liu J 2013 *Commun. Theor. Phys.* **60** 222

[19] Wang L, Hong X R, Sun J A, Tang R A, Yang Y, Zhou W J, Tian J M and Duan W S 2017 *Phys. Lett. A* **381** 2065

[20] Deng S H and Liu M P 2019 *Chin. Phys. B* **28** 044101

[21] Zhang S, Xie B S, Hong X R, Wang H C and Zhao X Y 2011 *Phys. Plasmas* **18** 033104

[22] Hong X R, Xie B S, Zhang S, Wang H C and Zhao X Y 2011 *Phys. Plasmas* **18** 103106

[23] Mendonca J T and Vieira J 2014 *Phys. Plasmas* **21** 033107

[24] Vieira J and Mendonca J T 2014 *Phys. Rev. Lett.* **112** 215001

[25] Zhang X M, Shen B F, Zhang L G, Xu J C, Wang X F, Wang W P, Yi L G and Shi Y 2014 *New J. Phys.* **16** 123051

[26] Firouzjaei A S and Shokri B 2016 *Phys. Plasmas* **23** 063102

[27] Firouzjaei A S and Shokri B 2017 *Phys. Plasmas* **24** 013107

[28] Zhang G B, Chen M, Schroeder C B, Luo J, Zeng M, Li F Y, Yu L L, Weng S M, Ma Y Y, Yu T P, Sheng Z M and Esarey E 2016 *Phys. Plasmas* **23** 033114

[29] Shen Z C, Chen M, Zhang G B, Luo J, Weng S M, Yuan X H, Liu F and Sheng Z M 2017 *Chin. Phys. B* **26** 115204

[30] Zhu X L, Chen M, Yu T P, Weng S M, Hu L X, McKenna P and Sheng Z M 2018 *Appl. Phys. Lett.* **112** 174102

[31] Hu L X, Yu T P, Sheng Z M, Vieira J, Zou D B, Yin Y, McKenna P and Shao F Q 2018 *Sci. Rep.* **8** 7282

[32] Porras M A 2019 *Phys. Rev. Lett.* **122** 123904

[33] Wang W P, Jiang C, Shen B F, Yuan F, Gan Z M, Zhang H, Zhai S H and Xu Z Z 2019 *Phys. Rev. Lett.* **122** 024801

[34] Cormier-Michel E, Esarey E, Geddes C G R, Schroeder C B, Paul K, Mullowney P J, Cary J R and Leemans W P 2011 *Phys. Rev. ST Accel. Beams* **14** 031303

[35] Anderson D and Bonnedal M 1979 *Phys. Fluids* **22** 105

[36] Wang W M, Sheng Z M, Zeng M, Liu Y, Hu Z D, Kawata S, Zhang C Y, Mori W B, Chen L M, Li Y T and Zhang J 2012 *Appl. Phys. Lett.* **101** 184104

[37] Wang W M, Sheng Z M, Wilson T, Li Y T and Zhang J 2020 *Phys. Rev. E* **101** 011201(R)